Inorganic Chemistry

pubs.acs.org/IC

Article

Accessing Boron-Doped Pentaphene Analogues from 12-Boradibenzofluorene

Manjur O. Akram, John R. Tidwell, Jason L. Dutton, David J. D. Wilson, Andrew Molino, and Caleb D. Martin*

Cite This: *Inorg. Chem.* 2022, 61, 9595−9604

Read Online

ACCESS | Metrics & More | Article Recommendations | Supporting Information

ABSTRACT: Borole-doped polycyclic aromatic hydrocarbons (PAHs) have garnered attention in recent years due to their attractive photophysical properties and potential utility in electronic devices. In this work, a borole-doped PAH, 12-boradibenzofluorene, is synthesized and formal intermolecular nitrene and oxygen atom insertion reactions were employed to access 1,2-azaborine- and 1,2-oxaborine-containing analogues of the carbonaceous PAH pentaphene. Iodosobenzene is established as a versatile reagent for oxygen atom insertion reactions into a variety of borole species to access 1,2-oxaborine systems.

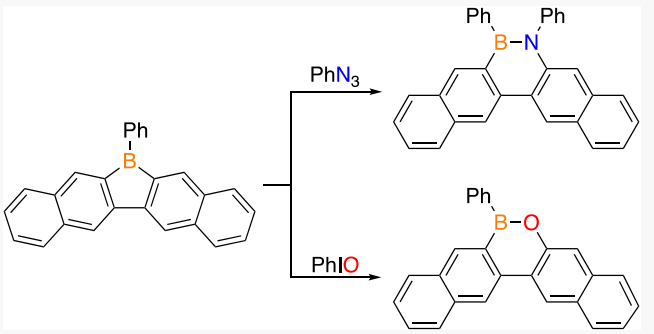

INTRODUCTION

Boroles are unsaturated five-membered heterocycles with four π-electrons and can be viewed as analogues to the cyclopentadienyl cation ($C_5H_5^+$) where one of the carbon atoms is replaced by a trigonal planar boron center (Figure 1).[1] The unsaturated BC_4 ring exhibits an antiaromatic character that enhances the Lewis acidity at boron and reactivity of the boracycle. Kinetic stabilization is necessary to prevent dimerization or decomposition in monocyclic species, and annulation of the BC_4 ring also serves as a means of attenuating reactivity.[2] Borole derivatives have been known since the 1960s including arene-fused boroles, such as 9-borafluorenes, that represent variants of boron-doped polycyclic aromatic hydrocarbons (PAHs), which have electronic and photophysical properties appealing for electronic materials.[3,4]

Boroles and their polycyclic variants not only have interesting electronic properties but can also serve as reagents to access larger ring systems via insertion into the endocyclic boron−carbon bond.[5,6] In particular, 1,1-insertion reactions generate six-membered aromatic boracycles if the inserted atom bears a lone pair. These BEC_4 aromatic heterocycles are analogues of benzene and are actively being studied for use in medicinal chemistry and electronic materials.[7] Unfortunately, there are synthetic challenges of incorporating B−N and B−O units into polyaromatic scaffolds in comparison to their carbonaceous counterparts. Recently, intermolecular nitrene insertion reactions of organic azides with boroles and 9-borafluorenes have been effective in accessing 1,2-azaborine ring systems (Scheme 1a).[8] In these reactions, the majority of the products are 1,2-azaborine systems formed from the insertion of a nitrene unit and expulsion of N_2 (**I**), but in rare cases, the γ-nitrogen atom of the azide reagent inserted to make diazene systems (**II**) or other products. In regard to oxygen atom insertion, pentaarylboroles undergo insertion with *N*-methylmorpholine *N*-oxide to furnish 1,2-oxaborines (Scheme 1b, **III**)[9] and 9-Mes-9-borafluorene reacted with molecular oxygen to access 9,10-oxaboraphenanthrene (Scheme 1c, **IV**).[10] To date, these methods have only been demonstrated with boroles or 9-borafluorenes leading to monocyclic and tricyclic PAH systems. Other polycyclic boroles are attractive targets as they could be reagents to access new boron-doped PAHs and have interesting electronic properties themselves. Here, we report the synthesis of a pentacyclic borole system, 12-boradibenzofluorene, and explore its reactivity to access boron-doped pentaphene analogues.

RESULTS AND DISCUSSION

An effective route to access antiaromatic BC_4 rings is via tin−boron transmetallation from a SnC_4 stannole precursor and a dihaloborane.[11] To prepare the dibromo intermediate precursor to the stannole, the literature procedure was followed.[12] Dibromo species **1** could be converted to the magnesium Grignard in situ and reacted with nBu$_2$SnCl$_2$ to

Received: March 21, 2022
Published: June 13, 2022

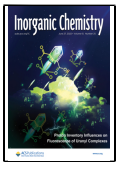

https://doi.org/10.1021/acs.inorgchem.2c00930
Inorg. Chem. 2022, 61, 9595−9604

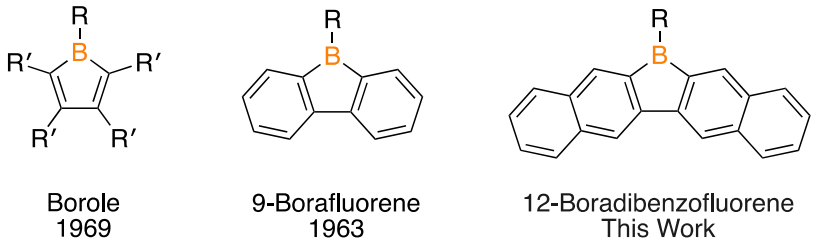

Figure 1. General structures of borole, 9-borafluorene, and targeted 12-boradibenzofluorene.

Scheme 1. Intermolecular Nitrene and Oxygen Insertion Reactions of Borole and 9-Borafluorenes to Access 1,2-Azaborine and 1,2-Oxaborine Systems[a]

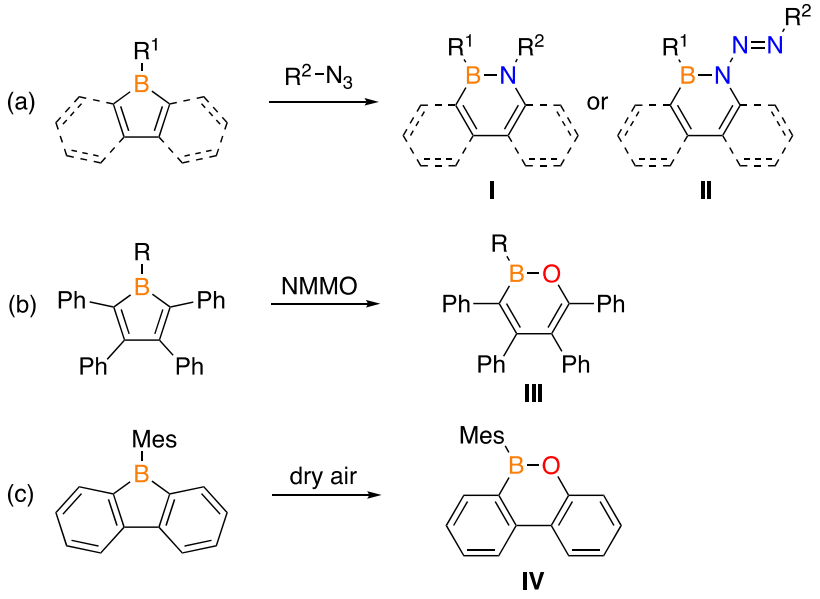

[a]NMMO, *N*-methylmorpholine *N*-oxide; Mes, 2,4,6-trimethylbenzene.

Scheme 2. Synthesis of 12-Boradibenzofluorene 3

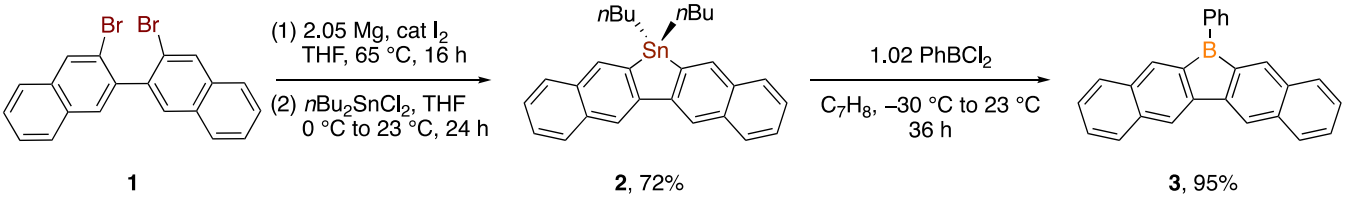

access stannole **2** in a 72% yield (Scheme 2). The target 12-boradibenzofluorene (**3**) was generated by tin−boron exchange between **2** and $PhBCl_2$ in a 95% yield as a yellow solid. The structures of **1**−**3** were determined by single-crystal X-ray diffraction studies (Figure S1 for **1** and Figure 2 for **2** and **3**).

In general, 9-borafluorenes are less Lewis acidic than the unfused parent species, boroles,[8g] and coordination has been reported to be the first mechanistic step for insertion into borole ring systems.[5] To determine if the extended conjugation in 12-boradibenzofluorene affects the Lewis acidity and insertion reactivity, we evaluated the Lewis acidity of **3** by the Gutmann−Beckett method.[13] Mixing a solution of **3** with $OPEt_3$ formed **3·OPEt$_3$** (Scheme 3), featuring a $^{31}P\{^1H\}$ NMR chemical shift of 74.0 ppm in $CDCl_3$, which translates to an acceptor number (AN) of 72.9.[14] The structure of **3·OPEt$_3$** was confirmed by a single-crystal X-ray diffraction study (Figure 2). The AN of **3** is lower than pentaphenylborole (80.4 in $CDCl_3$) but comparable to 9-Ph-9-borafluorene (73.6 in $CDCl_3$), suggesting that it is sufficiently Lewis acidic for insertion chemistry.

Reaction of **3** with 2 equivalents of phenyl azide at room temperature for 24 h only resulted in a 29% conversion based on ^1H NMR spectroscopy, but heating the reaction to 90 °C for 6 h resulted in the consumption of **3**.[15] Upon scale-up, the product was purified by flash column chromatography in the open atmosphere and was isolated in a 79% yield (Scheme 3). The structure of α-N insertion product **4** was determined by a single-crystal X-ray diffraction study (Figure 3).

Next, we attempted oxygen insertion reactions with **3** by following the existing protocols employed for pentaarylboroles and 9-Mes-9-borafluorene using *N*-methylmorpholine *N*-oxide and dry air, respectively.[9,10] In both reactions with **3**, complex mixtures were obtained with no conclusive evidence of 6,7-

https://doi.org/10.1021/acs.inorgchem.2c00930
Inorg. Chem. 2022, 61, 9595−9604

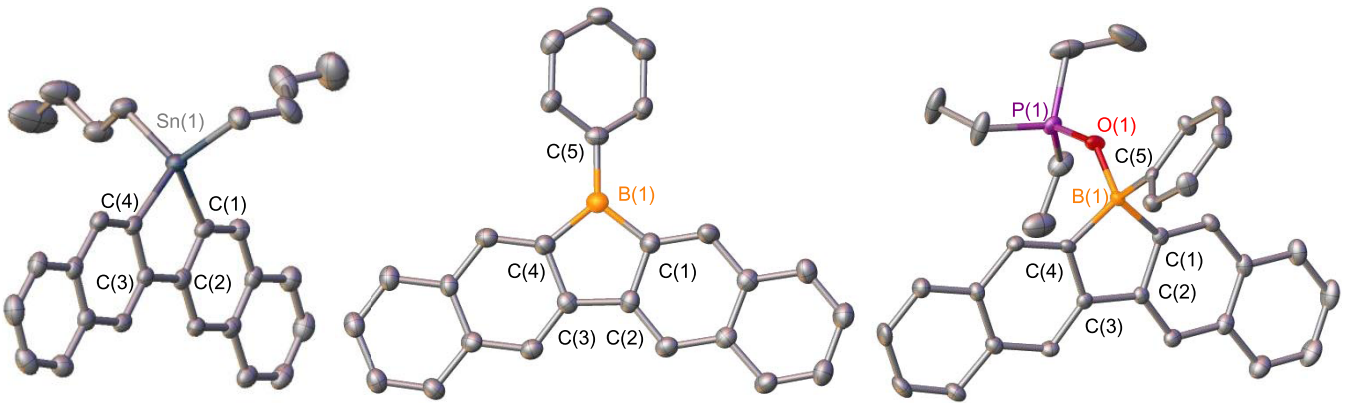

Figure 2. Solid-state structures of **2**, **3**, and **3·OPEt$_3$** (left to right). Hydrogen atoms are omitted for clarity, and thermal ellipsoids are drawn at the 50% probability level. Selected bond lengths (Å) and angles (°) of **2**: Sn(1)−C(1) 2.142(4), Sn(1)−C(4) 2.140(4), C(1)−C(2) 1.440 (6), C(2)−C(3) 1.499 (6), C(4)−C(3) 1.432(6), and C(1)−Sn(1)−C(4) 83.39(17); selected bond lengths (Å) and angles (°) of **3**: B(1)−C(1) 1.571(6), B(1)−C(4) 1.568(6), B(1)−C(5) 1.559(6), C(1)−C(2) 1.441(6), C(2)−C(3) 1.475(5), C(3)−C(4) 1.442(5), C(1)−B(1)−C(4) 104.0(3), C(1)−B(1)−C(5) 126.8(4), C(4)−B(1)−C(5) 129.1(4), B(1)−C(1)−C(2) 107.4(3), B(1)−C(4)−C(3) 107.9(3), C(1)−C(2)−C(3) 110.7(3), and C(2)−C(3)−C(4) 109.9(3); selected bond lengths (Å) and angles (°) of **3·OPEt$_3$**: B(1)−C(1) 1.626(4), B(1)−C(4) 1.625(4), B(1)−C(5) 1.613(4), B(1)−O(1) 1.561(4), C(1)−C(2) 1.434(4), C(2)−C(3) 1.480(4), C(3)−C(4) 1.436(4), O(1)−P(1) 1.521(2), C(1)−B(1)−C(4) 99.4(2), C(1)−B(1)−C(5) 110.3(2), C(1)−B(1)−O(1) 112.4(2), C(4)−B(1)−O(1) 113.4(3), C(4)−B(1)−C(5) 116.8(2), C(5)−B(1)−O(1) 104.8(2), B(1)−O(1)−P(1) 140.09(19), C(1)−C(2)−C(3) 110.4(3), and C(2)−C(3)−C(4) 110.3(3).

Scheme 3. Synthesis of Adduct 3·OPEt$_3$ and 6,7-Azaborapentaphene 4

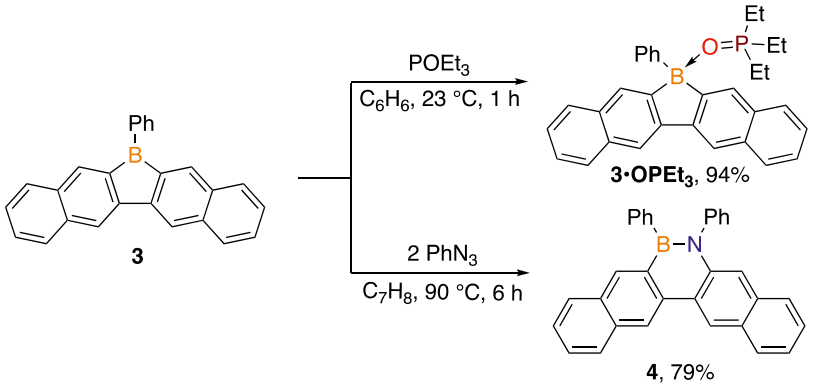

oxaborapentaphene (**5**) formation (Table 1, entries 1 and 2). Other oxygen atom donors were screened, namely, triethylamine *N*-oxide, pyridine-*N*-oxide, and the hypervalent iodine reagent tetra-*n*-butylammonium benziodoxolone,[16] but none were successful (Table 1, entries 3−5). All of these reagents provided complex reaction mixtures (Table 1, entries 1−5). We believe that the reagents or side products could form complexes or react further with **3** and **5**. The relatively mild oxidant dimethylsulfoxide produced the O-coordinated adduct cleanly (**3·DMSO**), which did not undergo further reactivity upon heating (Table 1, entry 6).[17] Gratifyingly, freshly prepared iodosobenzene[18] proved to be effective to access 6,7-oxaborapentaphene **5**, which was isolated in a 72% yield. Iodobenzene is the sole side product observed in this reaction, which did not react with either **3** or **5**. Despite numerous attempts, we could not grow single crystals of sufficient quality for X-ray diffraction studies. However, the pyridine adduct (**5·pyr**) could be prepared and the structure was confirmed by a single-crystal X-ray diffraction study (Figure 3). Interestingly, **4** is inert to pyridine, which is in line with theoretically calculated binding energies of pyridine to the boron center in **4** ($\Delta G°$ = +23.6 kJ mol^{-1}; Table S2) and **5** ($\Delta G°$ = −2.5 kJ mol^{-1}). Examination of the lowest unoccupied molecular orbital (LUMO) of **5** indicates a significant contribution from boron. Conversely, no contribution from boron is observed in the LUMO of **4**, highlighting the enhanced Lewis acidity of the boron center in **5** (Figures S69 and S70).

Nucleus-independent chemical shift (NICS) calculations were performed as a means to assess the aromatic character of **4** and **5**. Interestingly, the NICS(1)$_{ZZ}$ value for the azaborine (0.43 ppm) and oxaborine (2.84 ppm) central moieties in **4** and **5**, respectively, indicates a nonaromatic character according to NICS calculations (Figure 4). Expectedly, the annulated phenyl rings in both **4** and **5** were calculated to possess a significant aromatic character (NICS(1)$_{ZZ}$ = ∼ −26 ppm). These results contrast the calculated NICS(1)$_{ZZ}$ values for the dibenzo analogues of **4** (−7.1 ppm) and **5** (−3.1 ppm), which exhibit a minor-to-moderate aromatic character based on NICS values. This information initially suggested that **4** and **5** may be superaromatic systems possessing a peripheral macrocyclic conjugation. However, further analysis of the induced magnetic current density revealed two independent naphthalene moieties possessing diatropic ring-currents annulated to the 1,2-heteroborine ring (Figure 4). Although both azaborine and oxaborine moieties in **4** and **5** are formally aromatic according to Hückel's rule (6-π electrons), the

https://doi.org/10.1021/acs.inorgchem.2c00930
Inorg. Chem. 2022, 61, 9595−9604

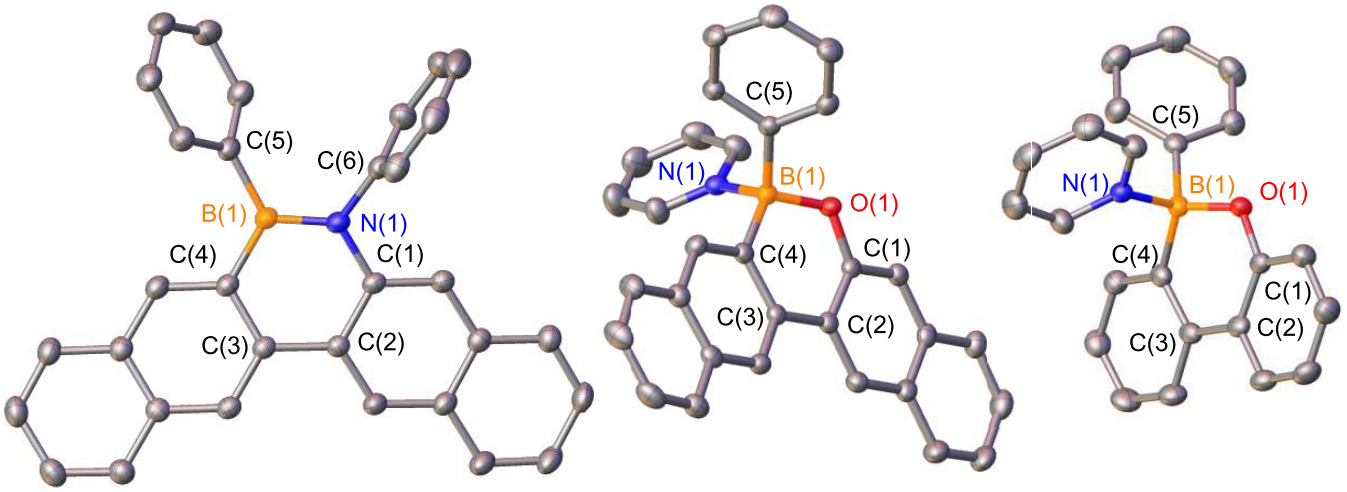

Figure 3. Solid-state structures of **4**, **5·pyr**, and **7·pyr** (left to right). Hydrogen atoms are omitted for clarity, and thermal ellipsoids are drawn at the 50% probability level. S− elected bond lengths (Å) and angles (°) of **4**: B(1)−N(1) 1.4223(18), B(1)−C(4) 1.5442(19), B(1)−C(5) 1.5730(19), N(1)−C(1) 1.4320(16), N(1)−C(6) 1.4532(16), C(1)−C(2) 1.4339(17), C(2)−C(3) 1.4758(17), C(3)−C(4) 1.4331(17), C(4)-B(1)−N(1) 116.93(11), C(4)−B(1)−C(5) 122.07(11), N(1)−B(1)−C(5) 120.82(11), B(1)−N(1)−C(1) 122.42(11), B(1)−N(1)−C(6) 122.28(10), C(1)−N(1)−C(6) 114.99(10), N(1)−C(1)−C(2) 119.42(11), C(1)−C(2)−C(3) 120.39(11), and C(2)−C(3)−C(4) 118.96(11); selected bond lengths (Å) and angles (°) of **5·pyr**: B(1)−O(1) 1.4632(18), B(1)−C(4) 1.610(12), B(1)−C(5) 1.614(2), B(1)−N(1) 1.6594(19), O(1)−C(1) 1.3551(16), C(1)−C(2) 1.4344(19), C(2)−C(3) 1.4799(19), C(3)−C(4) 1.4339(19), C(4)−B(1)−O(1) 112.42(12), C(4)−B(1)−C(5) 112.06(11), C(4)−B(1)−N(1) 110.75(11), O(1)−B(1)−C(5) 109.38(12), O(1)−B(1)−N(1) 104.56(11), C(5)−B(1)−N(1) 107.29(11), B(1)−O(1)−C(1) 119.30(12), O(1)−C(1)−C(2) 121.60(12), C(1)−C(2)−C(3) 120.01(12), and C(2)−C(3)−C(4) 118.58(12); selected bond lengths (Å) and angles (°) of **7·pyr**: B(1)−O(1) 1.470(2), B(1)−C(4) 1.600(2), B(1)−C(5) 1.614(2), B(1)−N(1) 1.672(2), O(1)−C(1) 1.3624(19), C(1)−C(2) 1.402(2), C(2)−C(3) 1.482(2), C(3)−C(4) 1.410(2), C(4)−B(1)−O(1) 112.18(13), C(4)−B(1)−C(5) 114.32(13), C(4)−B(1)−N(1) 108.31(12), O(1)−B(1)−C(5) 109.45(13), O(1)−B(1)−N(1) 103.67(12), C(5)−B(1)−N(1) 108.29(12), B(1)−O(1)−C(1) 121.98(11), O(1)−C(1)−C(2) 122.59(14), C(1)−C(2)−C(3) 120.30(14), and C(2)−C(3)−C(4) 118.61(14).

Table 1. Reactions Investigated to Synthesize 6,7-Oxaborapentaphene 5 from 3

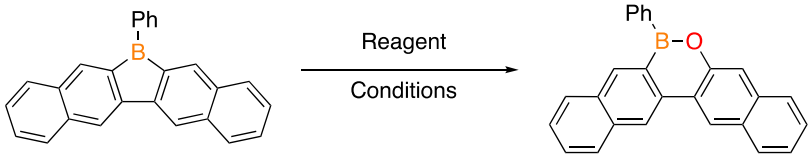

3 **5**

entry	reagent	reaction conditions	isolated yield of **5**
1	dry O_2	CH_2Cl_2, 23 °C, 16 h	[a]
2	NMMO	CH_2Cl_2, −78 to 23 °C, 1 h	[a]
3	$ONEt_3$	CH_2Cl_2, −78 to 23 °C, 1 h	[a]
4	pyridine-*N*-oxide	CH_2Cl_2, −78 to 23 °C, 1 h	[a]
5	[N*n*Bu$_4$] [benziodoxolone]	CH_2Cl_2, −30 to 23 °C, 2 h	[a]
6	DMSO	C_7H_8, 100 °C, 36 h	[b]
7	PhIO	CH_2Cl_2, 23 °C, 1 h	72%

[a]Complex reaction mixture was observed in ^{1}H and ^{11}B NMR spectroscopies. [b]Formation of **3·DMSO** (see the Experimental Section).

bonding in the central rings for these systems is localized based on the NICS data.

Prior routes to access 1,2-oxaborine systems were not universal, prompting us to examine the efficacy of iodosobenzene as an oxygen atom source to access 1,2-oxaborine systems from borole reagents. The corresponding oxygen insertion reactions with pentaphenylborole and 9-Ph-borafluorene generated pentaphenyl-1,2-oxaborine (**6**, Scheme 4)[9] and 9,10-oxaboraphenanthrene (**7**), respectively. The previously reported NMMO route to **6** is comparable in yield (66 vs 64%), and the yield for **7** using iodosobenzene is 74%, while the route using dry air to access 9,10-oxaboraphenanthrene **IV** did not have an isolated yield.[10] Although we could not obtain a single crystal of **7**, the corresponding pyridine-coordinated product **7·pyr** was synthesized and its structure was confirmed by single-crystal X-ray diffraction studies (Figure 3). The outcome of these reactions indicates that iodosobenzene is a versatile reagent for oxygen insertion reactions into boroles given the good yields, mild reaction conditions, and benign iodobenzene byproduct.

The connectivity of all insertion products has been confirmed by single-crystal X-ray diffraction studies. In **3** (Figure 2), both the endocyclic and exocyclic C−B bonds are similar in length [B(1)−C(5) 1.559(6) Å, B(1)−C(1) 1.571(6) Å, and B(1)−C(4) 1.568(6) Å], which elongated upon coordination by $OPEt_3$ [B(1)−C(1) 1.626(4) Å, B(1)−C(4) 1.625(4) Å, and B(1)−C(5) 1.613(4) Å] attributed to the disruption of conjugation in the central ring. The B−O

https://doi.org/10.1021/acs.inorgchem.2c00930
Inorg. Chem. 2022, 61, 9595−9604

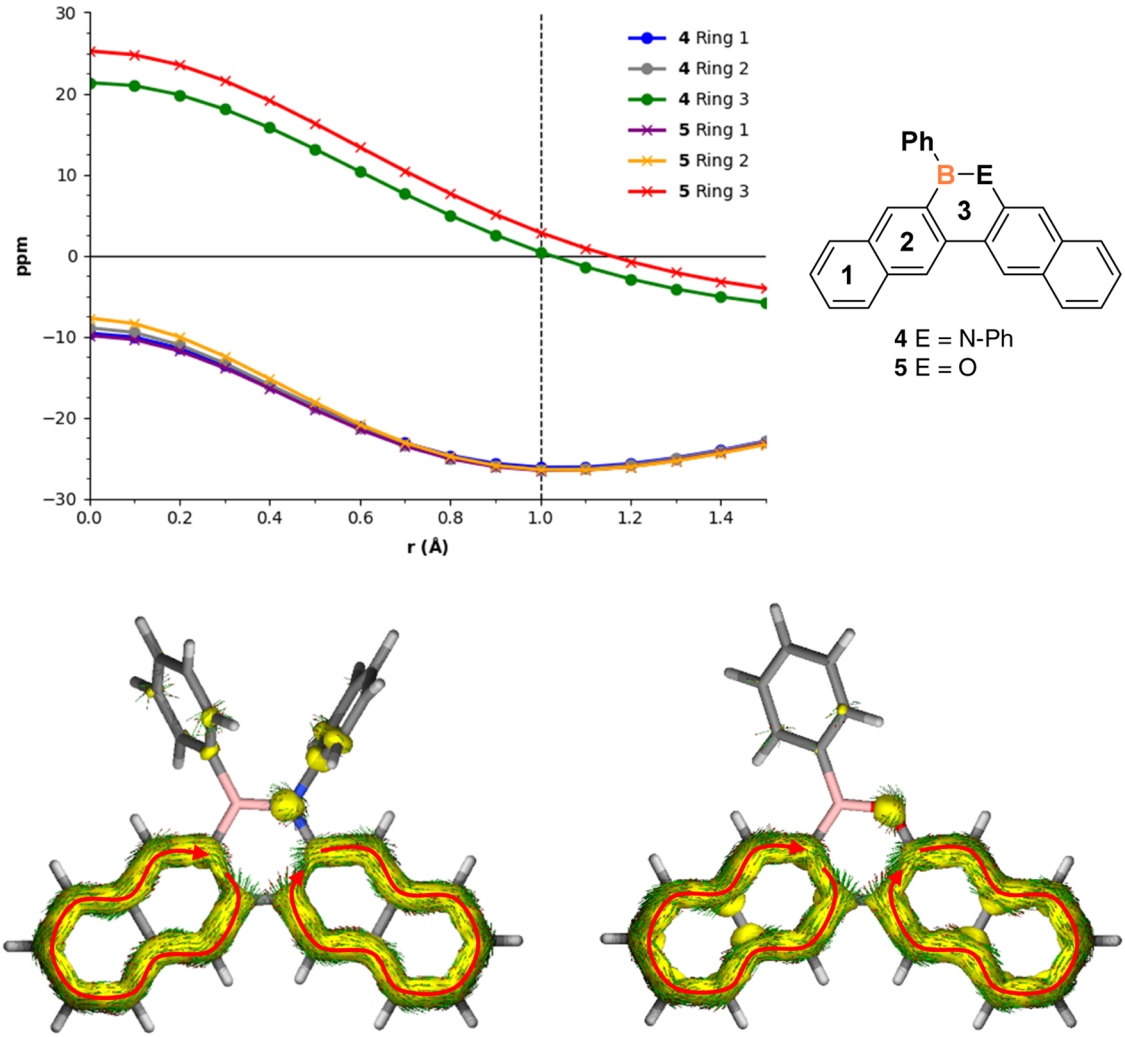

Figure 4. (a) Scan of the ZZ component of the nucleus-independent chemical shift ($NICS_{ZZ}$-scan). (b) ACID isosurface (0.04) of the π system of **4** (left) and **5** (right). The current vectors plotted onto the ACID isosurface indicate a strong diatropic ring current in the naphthalene moieties.

Scheme 4. Efficacy of Iodosobenzene as an Oxygen Insertion Reagent to Pentaphenylborole (a) and 9-Ph-9-Borafluorene (b)

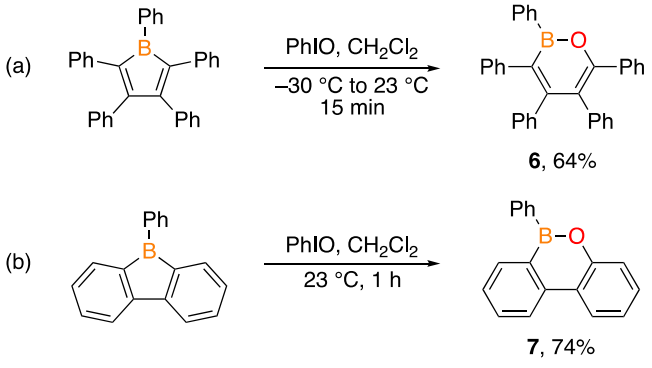

[1.561(4) Å] and the O–P [1.521(2) Å] bond lengths in **3·OPEt$_3$** are comparable to the corresponding 9-Ph-9-borafluorene–$OPEt_3$ adduct [B–O 1.567(4) Å and O–P 1.524(2) Å],[8g] which matches the similar Gutmann–Beckett values for Lewis acidity. The bond lengths in the central azaborine ring of **4** match those for monocyclic systems.[8g]

The photophysical properties of **3**–**5** and **7** were investigated by UV–vis and fluorescence spectroscopy (Table 2). In dichloromethane, compounds **3**–**5** and **7** have absorption maxima (λ_{abs}) at 310 nm ($\varepsilon = 6.8 \times 10^4$ M^{-1} cm^{-1}), 306 nm ($\varepsilon = 4.8 \times 10^4$ M^{-1} cm^{-1}), 301 nm ($\varepsilon = 3.8\times 10^4$ M^{-1} cm^{-1}), and 272 nm ($\varepsilon = 1.8 \times 10^4$ M^{-1} cm^{-1}), respectively. The emission maxima (λ_{em}, with Stokes shifts in parentheses) are 523 nm (1.3×10^4 cm^{-1}), 395 nm (7.4×10^3 cm^{-1}), 408

Table 2. Photophysical Properties of Compounds 3–5 and 7

compound	λ_{abs} (nm)	λ_{em} (nm)	ε^a (M^{-1} cm^{-1})	Stokes shift (cm^{-1})	$\Phi_n{}^b$
3	310	523	6.8×10^4	1.3×10^4	0.27[c]
4	306	395	4.8×10^4	7.4×10^3	0.51[d]
5	301	408	3.8×10^4	8.7×10^3	0.38[d]
7	272	360	1.8×10^4	9.0×10^3	0.21[e]

[a] ε is the molar extinction coefficient. [b] Φ_n is the fluorescence quantum yield. [c] Φ_3 is calculated in dichloromethane using quinine sulfate (quantum yield 0.546 in 0.5 M H_2SO_4) as a reference. [d] Φ_4 and Φ_5 are calculated in dichloromethane using anthracene (quantum yield 0.36 in cyclohexane) as a reference. [e] Φ_7 is calculated in dichloromethane using naphthalene (quantum yield 0.23 in cyclohexane) as a reference.

https://doi.org/10.1021/acs.inorgchem.2c00930
Inorg. Chem. 2022, 61, 9595–9604

nm (8.7×10^3 cm^{-1}), and 360 nm (9.0×10^3 cm^{-1}) for **3**–**5** and **7**, respectively. The Stokes shift of **3** is notably higher than that of the corresponding pentaphene (λ_{abs} 308 nm, $\lambda_{em} \sim 432$ nm, Stokes shift 9.3×10^3 cm^{-1} in cyclohexane).[19] The Stokes shifts for **4** and **5** are lower than those of pentaphene. The fluorescence quantum yields of compounds **3**–**5** and **7** are found to be 0.27 (reference: quinine sulfate), 0.51 (reference: anthracene), 0.38 (reference: anthracene), and 0.21 (reference: naphthalene), respectively, in dichloromethane.[20] Theoretical excitation and emission energies are in excellent agreement with experimental observations. The lowest-energy excitations in **3**–**5** and **7** indicate predominantly $\pi \rightarrow \pi^*$ transitions distributed throughout the PAH framework with oxaborines **5** and **7** exhibiting a minor charge-transfer character between the heterocycle and the phenyl group bound to boron (Figures S70 and S71).

CONCLUSIONS

In this work, a conjugated pentacyclic borole variant, 12-boradibenzofluorene, was prepared, which is a reagent to access hybrid boron–oxygen-containing analogues of pentaphene via intermolecular nitrene and oxygen atom insertion reactions, respectively. The hybrid organic/inorganic boron–oxygen-containing analogue of pentaphene, 6,7-oxaborapentaphene reacted with pyridine, while 6,7-azaborapentaphene did not, indicating increased Lewis acidity at boron and decreased aromaticity. Iodosobenzene proved to be an effective oxygen atom reagent for other borole systems, namely, pentaphenylborole and 9-Ph-9-borafluorene, based on good yields, mild reaction conditions, and benign iodobenzene byproduct.

EXPERIMENTAL SECTION

General Considerations. All manipulations were performed under an inert atmosphere in a nitrogen-filled MBraun Unilab glovebox or using standard Schlenk techniques unless specified. Chloroform-d and benzene-d^6 for NMR spectroscopy were purchased from Cambridge Isotope Laboratories, Inc., dried by stirring for 5 days over CaH_2, distilled, and stored over 4 Å molecular sieves. *m*-Xylene was dried in the same manner. All other solvents were purchased from commercial sources as anhydrous grade, dried further using a JC Meyer Solvent System with dual columns packed with solvent-appropriate drying agents, and stored over 3 or 4 Å molecular sieves. 2,3-Dibromonaphthalene, *n*BuLi, $n Bu_2SnCl_2$, Me_2SnCl_2, PhN_3, and $PhBCl_2$ were purchased from commercial sources and used without further purification. Mg metal turnings were purchased and activated with dilute HCl, washed with acetone, and dried before use. Pentaphenylborole and 9-Ph-9-borafluorene were prepared according to the literature procedure.[3c,11] Compound **1** was prepared, with the only modification being stirring the reaction for 24 h instead of 10 min.[12] The purity of new complexes was established by elemental analysis or multinuclear NMR (^1H, ^{11}B, $^{13}C\{^1H\}$); the spectra are available in the Supporting Information.

Multinuclear NMR spectra (^1H, $^{13}C\{^1H\}$, $^{31}P\{^1H\}$, ^{11}B, ^{119}Sn) were recorded on a Bruker Avance III HD 400 MHz or 600 MHz instrument. High-resolution mass spectra (HRMS) were obtained in the Baylor University Mass Spectrometry Center on a Thermo Scientific LTQ Orbitrap Discovery spectrometer using +ESI or at the University of Texas at Austin Mass Spectrometry Center using CI. Elemental (C, H, and N) analyses were performed by Atlantic Microlab, Inc. (Norcross, GA). Melting points were measured with a Thomas Hoover Uni-melt capillary melting point apparatus and are uncorrected. Fourier transform infrared (FT-IR) spectra were recorded on a Bruker Alpha ATR FT-IR spectrometer on solid samples. UV–vis and fluorescence data were collected on a Varian UV–vis spectrometer and a Fluoromax-4 fluorescence spectrometer, respectively. Single-crystal X-ray diffraction data were collected on a Bruker Apex III-CCD detector using Mo Kα radiation (λ = 0.71073 Å). Crystals were selected under paratone oil, mounted on MiTeGen micromounts, and immediately placed in a cold stream of N_2. Structures were solved and refined using SHELXTL, and figures were produced using OLEX2.[21]

2: A 250 mL two-necked flask fitted with a reflux condenser and a rubber septum was charged with magnesium turnings (16.02 mmol, 389.0 mg) and catalytic I_2 in tetrahydrofuran (THF) (20 mL). A THF solution (30 mL) of **1** (7.814 mmol, 3.200 g) was slowly added (over 1 h) to the reaction mixture via a syringe under refluxing conditions (65 °C) and heated for 16 h. The reaction mixture was cooled to −78 °C, and a THF solution (50 mL) of $n Bu_2SnCl_2$ (8.204 mmol, 2.490 g) was added slowly via a syringe. The cold bath was removed, and the reaction was allowed to warm to 23 °C and stirred for 24 h. Water (20 mL) was added, and the reaction mixture was extracted with ethyl acetate (2 × 30 mL). The collected organic layer was dried over Na_2SO_4, and the volatiles were removed in vacuo. The residue was purified by silica gel flash column chromatography using NEt_3/hexanes (1:20) as an eluant to afford **2** in a 72% yield. Single crystals for X-ray diffraction studies were by vapor diffusion of a CH_2Cl_2 solution of **2** into *m*-xylene. R_f: 0.75 (hexanes); yield: 72%, 2.750 g; physical appearance: white solid; mp: 98–101 °C; ^1H NMR (400 MHz, $CDCl_3$): δ = 8.62 (s, 2H, $Ar_{C\text{-}H}$), 8.17 (s, 2H, $Ar_{C\text{-}H}$), 7.96 (d, J = 7.6 Hz, 2H, $Ar_{C\text{-}H}$), 7.84 (d, J = 7.6 Hz, 2H, $Ar_{C\text{-}H}$), 7.49 (p, J = 6.7 Hz, 4H, $Ar_{C\text{-}H}$), 1.80–1.49 (m, 4H, CH_2), 1.54–1.26 (m, 8H, -CH_2-CH_2-), 0.88 (t, J = 7.3 Hz, 6H, -CH_3) ppm; $^{13}C\{^1H\}$ NMR (101 MHz, $CDCl_3$): δ = 145.6 ($C_{quat.}$), 140.3 ($C_{quat.}$), 136.9 (t, J = 20.2 Hz, $Ar_{C\text{-}H}$), 134.4 ($C_{quat.}$), 133.4 ($C_{quat.}$), 128.7 ($Ar_{C\text{-}H}$), 127.6 ($Ar_{C\text{-}H}$), 126.3 ($Ar_{C\text{-}H}$), 125.9 ($Ar_{C\text{-}H}$), 121.3 (t, J = 16.1 Hz, $Ar_{C\text{-}H}$), 29.2 (t, J = 12.1 Hz, -CH_2-), 27.3 (t, J = 28.3 Hz, -CH_2-), 13.8 (-CH_3), 12.7 (dt, J = 180.8 Hz, 8.1 Hz, -CH_2-) ppm; ^{119}Sn NMR (149 MHz, $CDCl_3$): δ = −35.1 ppm; FT-IR (ranked intensity, cm^{-1}): 2914 (5), 1490 (13), 1461 (8), 1313 (11), 1189 (9), 943 (10), 874 (3), 842 (12), 740 (1), 689 (6), 658 (15) 628 (14), 594 (7), 512 (4), 471 (2); HRMS (ESI): calcd 487.1422 for $C_{28}H_{30}Sn$ $[M + H]^+$, found 487.1443.

3: In a glovebox, dichlorophenylborane (1.890 mmol, 245.0 μL) was added to a solution of **2** (1.850 mmol, 900.0 mg) in toluene (15 mL) over a period of 5 min at −30 °C. The reaction mixture was allowed to warm to 23 °C and stirred for 60 h. The solution was concentrated in vacuo to a volume of ∼2 mL, and *n*-pentane (20 mL) was added. The reaction mixture was stirred for 1 h and filtered to collect a yellow powder, which was dried in vacuo to obtain **3**. Single crystals for X-ray diffraction studies were grown from a CH_2Cl_2 solution of **3** by vapor diffusion into toluene. Yield: 95%, 600.0 mg; physical appearance: yellow solid; mp: 204–206 °C; ^1H NMR (400 MHz, $CDCl_3$): δ = 8.39 (s, 2H, $Ar_{C\text{-}H}$), 8.32–8.26 (m, 2H, $Ar_{C\text{-}H}$), 8.06 (s, 2H, $Ar_{C\text{-}H}$), 7.87–7.80 (m, 4H, $Ar_{C\text{-}H}$), 7.68–7.63 (m, 3H, $Ar_{C\text{-}H}$), 7.51 (ddd, J = 8.1, 6.9, 1.3 Hz, 2H, $Ar_{C\text{-}H}$), 7.41 (ddd, J = 8.1, 6.9, 1.3 Hz, 2H, $Ar_{C\text{-}H}$) ppm; $^{13}C\{^1H\}$ NMR (101 MHz, $CDCl_3$): δ = 148.8 ($C_{quat.}$), 137.5 ($C_{quat.}$), 137.3 ($Ar_{C\text{-}H}$), 135.6 ($Ar_{C\text{-}H}$), 134.2 ($Ar_{C\text{-}H}$), 131.8 ($C_{quat.}$), 130.5 ($Ar_{C\text{-}H}$), 128.7 ($Ar_{C\text{-}H}$), 128.6 ($Ar_{C\text{-}H}$), 128.5 ($Ar_{C\text{-}H}$), 126.2 ($Ar_{C\text{-}H}$), 118.7 ($Ar_{C\text{-}H}$) ppm; ^{11}B NMR (193 MHz, $CDCl_3$): δ = 63.7 ppm; FT-IR (ranked intensity, cm^{-1}): 1627 (14), 1594 (6), 1493 (13), 1445 (9), 1315 (10), 1292 (5), 1144 (12), 1112 (8), 981 (15), 872 (2), 737 (1), 691 (4), 590 (7), 517 (11), 469 (3); HRMS (CI): calcd 341.1499 for $C_{26}H_{18}B$ $[M + H]^+$, found 341.1499; elemental analysis: calcd C 91.99, H 5.04 for $C_{26}H_{17}B$; found: C 91.39, H 5.11.

3·OPEt$_3$: Triethylphosphine oxide (0.20 mmol, 27.0 mg) in benzene (2 mL) was added slowly at 23 °C to a solution of **3** (0.20 mmol, 68.0 mg) in benzene (4 mL) and stirred for 1 h. The volatiles were removed in vacuo, and the residue was washed with cold *n*-pentane (2 × 2 mL) and dried in vacuo to obtain **3·OPEt$_3$**. Single crystals for X-ray diffraction studies were grown by vapor diffusion of a CH_2Cl_2 solution of **3·OPEt$_3$** into toluene. Yield: 94%, 89 mg; physical appearance: white solid; mp: 156–159 °C; ^1H NMR (400 MHz, $CDCl_3$): δ = 8.16 (s, 2H, $Ar_{C\text{-}H}$), 7.86 (s, 2H, $Ar_{C\text{-}H}$), 7.80 (dd, J = 8.3, 1.4 Hz, 2H, $Ar_{C\text{-}H}$), 7.65 (dd, J = 8.0, 1.4 Hz, 2H, $Ar_{C\text{-}H}$), 7.48 (d, J = 7.0 Hz, 2H, $Ar_{C\text{-}H}$), 7.30 (ddd, J = 13.6, 6.1, 1.5 Hz, 3H, $Ar_{C\text{-}H}$), 7.27–7.24 (m, 1H, $Ar_{C\text{-}H}$), 7.18–7.13 (m, 2H, $Ar_{C\text{-}H}$), 7.10–

https://doi.org/10.1021/acs.inorgchem.2c00930
Inorg. Chem. 2022, 61, 9595–9604

7.04 (m, 1H, $Ar_{C\text{-}H}$), 1.46 (dq, J = 12.1, 7.7 Hz, 6H, -CH_2-), 0.89 (dt, J = 17.6, 7.7 Hz, 9H, -CH_3) ppm; $^{13}C\{^1H\}$ NMR (101 MHz, $CDCl_3$): δ = 147.3 ($C_{quat.}$), 134.5 ($C_{quat.}$), 134.4 ($Ar_{C\text{-}H}$), 131.9 ($Ar_{C\text{-}H}$), 130.8 ($C_{quat.}$), 128.5 ($C_{quat.}$), 128.4 ($Ar_{C\text{-}H}$), 128.3 ($Ar_{C\text{-}H}$), 127.2 ($Ar_{C\text{-}H}$), 125.5 ($C_{quat.}$), 125.2 ($Ar_{C\text{-}H}$), 124.7 ($Ar_{C\text{-}H}$), 117.7 ($Ar_{C\text{-}H}$), 17.6 (d, J = 65.6 Hz, -CH_2-), 5.5 (d, J = 4.9 Hz, -CH_3) ppm; $^{31}P\{^1H\}$ NMR (162 MHz, $CDCl_3$): δ = 74.0 ppm; ^{11}B NMR (128 MHz, $CDCl_3$): δ = 8.4 ppm; FT-IR (ranked intensity, cm^{-1}): 1490 (10), 1420 (9), 1322 (13), 1179 (8), 1137 (12),1057 (15), 1031 (11), 894 (3), 862 (7), 793 (6), 759 (14), 728 (1), 707 (4), 611 (5), 479 (2).

3·DMSO: Dimethylsulfoxide (0.20 mmol, 7.1 μL) was added to a solution of **3** (0.10 mmol, 34 mg) in toluene (4 mL) at 23 °C and stirred for 15 min. The volatiles were removed in vacuo, and the product was recrystallized from DCM/*n*-pentane (1:9). The powder was dried in vacuo to obtain **3·DMSO**. Yield: 88%, 37 mg; physical appearance: white solid; mp: 178−181 °C; ^1H NMR (400 MHz, $CDCl_3$): δ = 8.24 (s, 2H, $Ar_{C\text{-}H}$), 8.06 (s, 2H, $Ar_{C\text{-}H}$), 7.91−7.84 (m, 2H, $Ar_{C\text{-}H}$), 7.78 (dd, J = 7.9, 1.4 Hz, 2H, $Ar_{C\text{-}H}$), 7.75−7.68 (m, 2H, $Ar_{C\text{-}H}$), 7.44−7.29 (m, 6H, $Ar_{C\text{-}H}$), 7.25−7.21 (m, 1H, $Ar_{C\text{-}H}$), 2.55 (s, 6H, -CH_3); $^{13}C\{^1H\}$ NMR (101 MHz, $CDCl_3$): δ = 147.6 ($C_{quat.}$), 135.0 ($C_{quat.}$), 134.3 ($C_{quat.}$), 132.7 ($Ar_{C\text{-}H}$), 131.5 ($Ar_{C\text{-}H}$), 128.6 ($Ar_{C\text{-}H}$), 128.4 ($Ar_{C\text{-}H}$), 127.6 ($Ar_{C\text{-}H}$), 126.8 ($C_{quat.}$), 125.8 ($Ar_{C\text{-}H}$), 125.1 ($Ar_{C\text{-}H}$), 118.0 ($Ar_{C\text{-}H}$), 38.7 (-CH_3); ^{11}B NMR (193 MHz, $CDCl_3$): δ = 16.4 ppm; FT-IR (ranked intensity, cm^{-1}): 1490 (10), 1420 (8), 1322 (13), 1137 (12), 1056 (4), 947 (14), 893 (3), 862 (9), 792 (7), 726 (1), 707 (6), 665 (11), 612 (5), 524 (15), 478 (2).

4: A solution of phenyl azide (0.80 mmol, 95 mg) in toluene (2 mL) was added to a solution of **3** (0.400 mmol, 136.0 mg) in toluene (4 mL) in a pressure tube. The reaction was heated at 90 °C for 6 h. The volatiles were removed in vacuo, and the residue was purified by silica gel flash column chromatography using CH_2Cl_2/hexanes (1:10) as the eluant to afford **4**. Caution: phenyl azides are potentially explosive. Although we never experienced any accidents during these studies, all of the experiments were carried out behind a safety shield in a fume hood. Single crystals for X-ray diffraction studies were grown by vapor diffusion of a chloroform solution of **4** into toluene. Yield: 79%, 137 mg; physical appearance: white solid; mp: 223−227 °C; ^1H NMR (400 MHz, $CDCl_3$): δ = 9.05 (s, 1H, $Ar_{C\text{-}H}$), 9.01 (s, 1H, $Ar_{C\text{-}H}$), 8.27 (s, 1H, $Ar_{C\text{-}H}$), 8.04 (d, J = 8.3 Hz, 1H, $Ar_{C\text{-}H}$), 7.99−7.94 (m, 1H, $Ar_{C\text{-}H}$), 7.81 (d, J = 8.2 Hz, 1H, $Ar_{C\text{-}H}$), 7.53 (ddd, J = 8.3, 4.5, 1.4 Hz, 2H, $Ar_{C\text{-}H}$), 7.41 (ddd, J = 8.1, 6.8, 1.2 Hz, 1H, $Ar_{C\text{-}H}$), 7.38−7.32 (m, 2H, $Ar_{C\text{-}H}$), 7.31−7.20 (m, 5H, $Ar_{C\text{-}H}$), 7.19−7.14 (m, 3H, $Ar_{C\text{-}H}$), 7.13−7.08 (m, 3H, $Ar_{C\text{-}H}$) ppm; $^{13}C\{^1H\}$ NMR (101 MHz, $CDCl_3$): δ = 144.4 ($C_{quat.}$), 141.5 ($C_{quat.}$), 139.5 ($Ar_{C\text{-}H}$), 135.1 ($C_{quat.}$), 135.1 ($C_{quat.}$), 133.1 ($C_{quat.}$), 133.0 ($Ar_{C\text{-}H}$), 132.3 ($C_{quat.}$), 129.9 ($Ar_{C\text{-}H}$), 129.4 ($Ar_{C\text{-}H}$), 129.3 ($C_{quat.}$), 128.9 ($Ar_{C\text{-}H}$), 128.4 ($Ar_{C\text{-}H}$), 128.0 ($Ar_{C\text{-}H}$), 127.6 ($Ar_{C\text{-}H}$), 127.2 ($Ar_{C\text{-}H}$), 127.2 ($Ar_{C\text{-}H}$), 127.1 ($Ar_{C\text{-}H}$), 127.0 ($Ar_{C\text{-}H}$), 126.4 ($Ar_{C\text{-}H}$), 125.9 ($Ar_{C\text{-}H}$), 125.5 ($C_{quat.}$), 124.7 ($Ar_{C\text{-}H}$), 123.7 ($Ar_{C\text{-}H}$), 121.1 ($Ar_{C\text{-}H}$), 115.4 ($Ar_{C\text{-}H}$) ppm; FT-IR (ranked intensity, cm^{-1}): 1626 (14), 1594 (6), 1493 (13), 1445 (9), 1315 (10), 1292 (5), 1144 (12), 1112 (8), 981 (15), 872 (2), 737 (1), 691 (4), 590 (7), 517 (11), 496 (3); HRMS (ESI): calcd 432.1918 for $C_{32}H_{22}BN$ $[M + H]^+$, found 432.1922.

*Preparation of **5** and **7**.* A dichloromethane solution containing 0.40 mmol of boron reagent (**3** for the synthesis of **5** or 9-Ph-9-borafluorene for the synthesis of **7**) was added dropwise to a dichloromethane solution of freshly prepared iodosobenzene (0.40 mmol, 88 mg), and the mixture was stirred at 23 °C for 1 h. The volatiles were removed in vacuo, and the residue was dissolved in a minimum amount of dichloromethane and loaded on a pipette silica column. First, 10 mL of *n*-pentane was used as an eluent to remove iodobenzene; then, 20 mL of 20% dichloromethane/pentane was employed as an eluent to collect **5** or **7**. Removal of the volatiles under vacuum gave the products.

*Characterization of **5**.* Yield: 72%, 103 mg; physical appearance: white solid; mp: 157−161 °C; ^1H NMR (400 MHz, $CDCl_3$): δ = 8.87 (br. s, 3H, $Ar_{C\text{-}H}$), 8.21−8.15 (m, 2H, $Ar_{C\text{-}H}$), 8.10−7.98 (m, 3H, $Ar_{C\text{-}H}$), 7.93 (s, 1H, $Ar_{C\text{-}H}$), 7.88 (d, J = 7.8 Hz, 1H, $Ar_{C\text{-}H}$), 7.69−7.59 (m, 4H, $Ar_{C\text{-}H}$), 7.53 (dt, J = 21.9, 7.6 Hz, 3H, $Ar_{C\text{-}H}$) ppm; $^{13}C\{^1H\}$ NMR (101 MHz, $CDCl_3$): δ = 149.5 ($C_{quat.}$), 140.2 ($Ar_{C\text{-}H}$), 135.8 ($C_{quat.}$), 134.7 ($Ar_{C\text{-}H}$), 134.7 ($C_{quat.}$), 134.0 ($C_{quat.}$), 132.5 ($C_{quat.}$), 130.6 ($Ar_{C\text{-}H}$), 130.3 ($C_{quat.}$), 129.3 ($Ar_{C\text{-}H}$), 128.5 ($Ar_{C\text{-}H}$), 128.4 ($Ar_{C\text{-}H}$), 128.3 ($Ar_{C\text{-}H}$), 128.2 ($Ar_{C\text{-}H}$), 127.1 ($Ar_{C\text{-}H}$), 126.7 ($Ar_{C\text{-}H}$), 126.4 ($Ar_{C\text{-}H}$), 125.1 ($Ar_{C\text{-}H}$), 124.1 ($C_{quat.}$), 123.3 ($Ar_{C\text{-}H}$), 121.1 ($Ar_{C\text{-}H}$), 116.2 ($Ar_{C\text{-}H}$) ppm; ^{11}B NMR (128 MHz, $CDCl_3$): δ = 43.7 ppm; FT-IR (ranked intensity, cm^{-1}): 1621 (15), 1592 (7), 1459 (6), 1430 (12), 1332 (14), 1287 (1), 1057 (9), 982 (11), 906 (13), 865 (4), 742 (2), 700 (5), 611 (8), 563 (10), 472 (3); HRMS (CI): calcd 356.1372 for $C_{26}H_{17}BO$ $[M + H]^+$, found 356.1366.

*Characterization of **7**.* Yield: 74%, 76 mg; physical appearance: white solid; mp: 89−93 °C; ^1H NMR (400 MHz, $CDCl_3$): δ = 8.43−8.34 (m, 2H, $Ar_{C\text{-}H}$), 8.30 (dd, J = 8.1, 1.6 Hz, 1H, $Ar_{C\text{-}H}$), 8.10−8.06 (m, 2H, $Ar_{C\text{-}H}$), 7.82 (ddd, J = 8.3, 7.2, 1.5 Hz, 1H, $Ar_{C\text{-}H}$), 7.61−7.52 (m, 5H, $Ar_{C\text{-}H}$), 7.49 (ddd, J = 8.3, 7.1, 1.6 Hz, 1H, $Ar_{C\text{-}H}$), 7.35 (ddd, J = 8.3, 7.1, 1.4 Hz, 1H, $Ar_{C\text{-}H}$) ppm; $^{13}C\{^1H\}$ NMR (101 MHz, $CDCl_3$): δ = 151.6 ($C_{quat.}$), 139.6 ($C_{quat.}$), 137.5 ($Ar_{C\text{-}H}$), 134.7 ($Ar_{C\text{-}H}$), 133.1 ($Ar_{C\text{-}H}$), 130.4 ($Ar_{C\text{-}H}$), 129.3 ($Ar_{C\text{-}H}$), 128.1 ($Ar_{C\text{-}H}$), 127.3 ($Ar_{C\text{-}H}$), 123.6 ($Ar_{C\text{-}H}$), 123.5 ($Ar_{C\text{-}H}$), 123.3 ($C_{quat.}$), 122.0 ($Ar_{C\text{-}H}$), 120.6 ($Ar_{C\text{-}H}$) ppm; ^{11}B NMR (128 MHz, $CDCl_3$): δ = 42.0 ppm; FT-IR (ranked intensity, cm^{-1}): 1598 (12), 1484 (7), 1446 (5), 1431 (15), 1284 (2), 1122 (14), 914 (8), 762 (10), 740 (3), 719 (6), 701 (1), 631 (4), 615 (9), 562 (13), 429 (11); HRMS (CI): calcd 256.1059 for $C_{18}H_{13}BO$ $[M]^+$, found 256.1059; elemental analysis: calcd C 84.42, H 5.12 for $C_{18}H_{13}BO$; found: C 83.58, H 5.36.

*Preparation of **5·pyr** and **7·pyr**.* Neat pyridine (0.80 mmol, 64 μL) was added via a micropipette at 23 °C to a dichloromethane solution containing 0.20 mmol of **5** or **7** (2 mL). The reaction mixture was stirred for 1 h, and the volatiles were removed in vacuo to give the products. Single crystals for X-ray diffraction studies were grown by vapor diffusion of a CH_2Cl_2 solution **5·pyr** into toluene.

*Characterization of **5·pyr**.* Single crystals for X-ray diffraction studies were grown by vapor diffusion of a CH_2Cl_2 solution **5·pyr** into toluene. Yield: 98%, 85 mg; physical appearance: white solid; mp: 149−152 °C; ^1H NMR (400 MHz, $CDCl_3$): δ = 8.59 (dt, J = 4.8, 1.6 Hz, 3H, $Ar_{C\text{-}H}$), 8.48 (s, 1H, $Ar_{C\text{-}H}$), 8.41 (s, 1H, $Ar_{C\text{-}H}$), 7.89 (d, J = 8.1 Hz, 1H, $Ar_{C\text{-}H}$), 7.79−7.68 (m, 4H, $Ar_{C\text{-}H}$), 7.61 (d, J = 8.1 Hz, 1H, $Ar_{C\text{-}H}$), 7.44 (s, 1H, $Ar_{C\text{-}H}$), 7.40 (ddd, J = 8.2, 6.8, 1.5 Hz, 1H, $Ar_{C\text{-}H}$), 7.37−7.34 (m, 1H, $Ar_{C\text{-}H}$), 7.33−7.25 (m, 6H, $Ar_{C\text{-}H}$), 7.24−7.17 (m, 2H, $Ar_{C\text{-}H}$) ppm; $^{13}C\{^1H\}$ NMR (101 MHz, $CDCl_3$): δ = 154.3 ($C_{quat.}$), 147.7 ($Ar_{C\text{-}H}$), 138.7 ($Ar_{C\text{-}H}$), 135.0 ($C_{quat.}$), 134.8 ($C_{quat.}$), 133.8 ($Ar_{C\text{-}H}$), 133.8 ($Ar_{C\text{-}H}$), 132.9 ($C_{quat.}$), 132.4 ($Ar_{C\text{-}H}$), 128.8 ($C_{quat.}$), 128.2 ($Ar_{C\text{-}H}$), 128.1 ($Ar_{C\text{-}H}$), 127.9 ($Ar_{C\text{-}H}$), 127.6 ($Ar_{C\text{-}H}$), 127.5 ($C_{quat.}$), 126.6 ($Ar_{C\text{-}H}$), 126.1 ($Ar_{C\text{-}H}$), 125.8 ($Ar_{C\text{-}H}$), 125.5 ($Ar_{C\text{-}H}$), 124.7 ($Ar_{C\text{-}H}$), 123.6 ($Ar_{C\text{-}H}$), 123.1 ($Ar_{C\text{-}H}$), 121.4 ($Ar_{C\text{-}H}$), 114.4 ($Ar_{C\text{-}H}$) ppm; ^{11}B NMR (128 MHz, $CDCl_3$): δ = 7.9 ppm; FT-IR (ranked intensity, cm^{-1}): 1597 (9), 1484 (8), 1446 (15), 1430 (5), 1257 (2), 1070 (12), 997 (13), 911 (7), 739 (3), 719 (10), 701 (1), 631 (14), 615 (4), 565 (11), 476 (6).

*Characterization of **7·pyr**.* Single crystals for X-ray diffraction studies were grown from a CH_2Cl_2 solution of **7·pyr** by vapor diffusion into toluene. Yield: 95%, 64 mg; physical appearance: white solid; mp: 160−162 °C; ^1H NMR (400 MHz, $CDCl_3$): δ = 8.63 (ddt, J = 5.1, 3.5, 1.6 Hz, 2H, $Ar_{C\text{-}H}$), 8.00 (dd, J = 7.9, 3.2 Hz, 1H, $Ar_{C\text{-}H}$), 7.97−7.93 (m, 1H, $Ar_{C\text{-}H}$), 7.85 (ddt, J = 9.5, 5.8, 1.8 Hz, 1H, $Ar_{C\text{-}H}$), 7.63−7.58 (m, 1H, $Ar_{C\text{-}H}$), 7.49 (ddt, J = 8.4, 6.9, 2.4 Hz, 1H, $Ar_{C\text{-}H}$), 7.46−7.40 (m, 4H, $Ar_{C\text{-}H}$), 7.38−7.29 (m, 4H, $Ar_{C\text{-}H}$), 7.28−7.22 (m, 2H, $Ar_{C\text{-}H}$), 7.00 (ddd, J = 8.2, 5.4, 3.4 Hz, 1H, $Ar_{C\text{-}H}$) ppm; $^{13}C\{^1H\}$ NMR (101 MHz, $CDCl_3$): δ = 154.4 ($C_{quat.}$), 146.7 ($Ar_{C\text{-}H}$), 139.5 ($Ar_{C\text{-}H}$), 137.2 ($C_{quat.}$), 134.9 ($Ar_{C\text{-}H}$), 132.9 ($Ar_{C\text{-}H}$), 129.1 ($Ar_{C\text{-}H}$), 128.8 ($Ar_{C\text{-}H}$), 127.6 ($Ar_{C\text{-}H}$), 127.3 ($Ar_{C\text{-}H}$), 126.8 ($Ar_{C\text{-}H}$), 125.0 ($Ar_{C\text{-}H}$), 124.8 ($C_{quat.}$), 123.8 ($Ar_{C\text{-}H}$), 121.9 ($Ar_{C\text{-}H}$), 120.4 ($Ar_{C\text{-}H}$), 120.1 ($Ar_{C\text{-}H}$) ppm; ^{11}B NMR (128 MHz, $CDCl_3$): δ = 14.6 ppm; FT-IR (ranked intensity, cm^{-1}): 1600 (8), 1483 (6), 1446 (15), 1430 (4), 1252 (2), 1122 (12), 1069 (9), 996 (11), 914 (7), 740 (5), 701 (1), 630 (14), 615 (3), 564 (13), 428 (10).

6: A dichloromethane solution of pentaphenylborole (0.10 mmol, 44 mg) was added dropwise to a dichloromethane (2 mL) solution of freshly prepared iodosobenzene (0.10 mmol, 22 mg) at −30 °C. The dark blue solution turned pale-yellow upon mixing. The bath was removed, and the reaction was allowed to warm to room temperature

https://doi.org/10.1021/acs.inorgchem.2c00930
Inorg. Chem. 2022, 61, 9595−9604

(23 °C) and stirred for an additional 15 min. The volatiles were removed in vacuo, and the residue was dissolved in a minimum amount of dichloromethane and loaded on a pipette silica column. First, 10 mL of *n*-pentane was used as an eluent to remove iodobenzene; then, 20 mL of 20% dichloromethane/pentane was employed as an eluent to collect **6**. Removal of the volatiles gave **6**. Solution ^{1}H, ^{11}B, and $^{13}C\{^{1}H\}$ NMR spectroscopies matched the literature values.[9] Yield: 64%, 30 mg.

THEORETICAL CALCULATIONS

Geometries were optimized using the B3LYP hybrid functional with dispersion corrections (D3(BJ)) and the def2-TZVP(−f) basis set using Orca 5.0.3.[22] All geometry optimizations included the CPCM solvation model with DCM or toluene solvent parameters.[23] All optimizations utilized the resolution of identity approximation for both Coulomb and Hartree−Fock exchange integrals and a 590-point integration grid. Harmonic frequency calculations were conducted analytically to confirm that optimized geometries were minima and to provide thermochemical data. Nucleus-independent chemical shift (NICS) scan calculations were performed using the Aroma plug-in package interfaced to Gaussian 16 at the B3LYP-D3(BJ)/6-311+G(d) level of theory.[24] Induced magnetic current densities were calculated using the continuous set of gauge transformation (CSGT) method of Bader et al. at the B3LYP-D3(BJ)/def2-TZVP level of theory and visualized using ACID 3.0.2.[25] Time-dependent density functional theory (TD-DFT) and excited-state dynamics (ESD) calculations were performed using ORCA 5.0.3. TD-DFT calculations were performed at the CAM-B3LYP-D3(BJ)/def2-TZVP//B3LYP-D3(BJ)/def2-TZVP(−f) level of theory using the CPCM solvation model with parameters for DCM.[26] Vibrationally resolved electronic spectra were calculated adiabatically utilizing Franck−Condon approximations from the reference STEOM-DLPNO-CCSD/def2-TZVP(−f) (CPCM, CH_2Cl_2)//B3LYP-D3(BJ)/def2-TZVP-(−f) excitation energies and transition dipole moments inclusive of the CPCM solvation model with parameters for DCM, with inhomogeneous line widths set to 300 cm^{-1}.[27]

ASSOCIATED CONTENT

Supporting Information

The Supporting Information is available free of charge at https://pubs.acs.org/doi/10.1021/acs.inorgchem.2c00930.

NMR spectra, photophysical spectra, FT-IR spectra, and theoretical calculations (PDF)

Accession Codes

CCDC 2159824−2159830 contain the supplementary crystallographic data for this paper. These data can be obtained free of charge via www.ccdc.cam.ac.uk/data_request/cif, or by emailing data_request@ccdc.cam.ac.uk, or by contacting The Cambridge Crystallographic Data Centre, 12 Union Road, Cambridge CB2 1EZ, UK; fax: +44 1223 336033.

AUTHOR INFORMATION

Corresponding Author

Caleb D. Martin − *Department of Chemistry and Biochemistry, Baylor University, Waco, Texas 76798, United States;* orcid.org/0000-0001-9681-0160; Email: caleb_d_martin@baylor.edu

Authors

Manjur O. Akram − *Department of Chemistry and Biochemistry, Baylor University, Waco, Texas 76798, United States*

John R. Tidwell − *Department of Chemistry and Biochemistry, Baylor University, Waco, Texas 76798, United States;* orcid.org/0000-0001-9216-7913

Jason L. Dutton − *Department of Biochemistry and Chemistry, La Trobe Institute for Molecular Science, La Trobe University, Melbourne 3086 Victoria, Australia;* orcid.org/0000-0002-0361-4441

David J. D. Wilson − *Department of Biochemistry and Chemistry, La Trobe Institute for Molecular Science, La Trobe University, Melbourne 3086 Victoria, Australia;* orcid.org/0000-0002-0007-4486

Andrew Molino − *Department of Biochemistry and Chemistry, La Trobe Institute for Molecular Science, La Trobe University, Melbourne 3086 Victoria, Australia;* orcid.org/0000-0002-0954-9054

Complete contact information is available at: https://pubs.acs.org/10.1021/acs.inorgchem.2c00930

Author Contributions

The manuscript was written through contributions of all authors. All authors have given approval to the final version of the manuscript.

Notes

The authors declare no competing financial interest.

ACKNOWLEDGMENTS

The authors are grateful to Baylor University, the Welch Foundation (Grant No. AA-1846), the National Science Foundation (Award No. 1753025), and the Australian Research Council (FT16010007 and DP20010013) for their generous support of this work. The authors thank Kristen Bluer for preliminary studies, Dr. Tyler Bartholome for assistance with X-ray crystallography, and Prof. Jung-Hyun Min, Dr. Suprakash Biswas, and Suresh Sunuwar for help with spectroscopic studies. Generous allocation of computing resources from National Computational Infrastructure (NCI), Intersect, and La Trobe University is acknowledged.

REFERENCES

(1) (a) Steffen, A.; Ward, R. M.; Jones, W. D.; Marder, T. B. Dibenzometallacyclopentadienes, boroles and selected transition metal and main group heterocyclopentadienes: Synthesis, catalytic and optical properties. *Coord. Chem. Rev.* **2010**, *254*, 1950−1976. (b) Braunschweig, H.; Kupfer, T. Recent developments in the chemistry of antiaromatic boroles. *Chem. Commun.* **2011**, *47*, 10903−10914. (c) Braunschweig, H.; Krummenacher, I.; Wahler, J. Chapter One—Free Boroles: The Effect of Antiaromaticity on Their Physical Properties and Chemical Reactivity. In *Advances in Organometallic Chemistry*, Hill, A. F.; Fink, M. J., Eds.; Academic Press, 2013; Vol. *61*, pp 1−53. (d) Zhang, W.; Zhang, B.; Yu, D.; He, G. Construction of highly antiaromatic boroles. *Sci. Bull.* **2017**, *62*, 899−900. (e) Nguyen, M. T.; van Trang, N.; Dung, T. N.; Nguyen, H. M. T. 3.18—Boroles. In *Comprehensive Heterocyclic Chemistry IV*, Black, D. S.; Cossy, J.; Stevens, C. V., Eds.; Elsevier, 2022; pp 833−873.

(2) (a) Fagan, P. J.; Nugent, W. A.; Calabrese, J. C. Metallacycle Transfer from Zirconium to Main Group Elements: A Versatile Synthesis of Heterocycles. *J. Am. Chem. Soc.* **1994**, *116*, 1880−1889. (b) Braunschweig, H.; Kupfer, T. Direct functionalization at the boron center of antiaromatic chloroborole. *Chem. Commun.* **2008**, 4487−4489. (c) Braunschweig, H.; Chiu, C.-W.; Damme, A.;

Ferkinghoff, K.; Kraft, K.; Radacki, K.; Wahler, J. Unwinding Antiaromaticity in 1-Bromo-2,3,4,5-tetraphenylborole. *Organometallics* **2011**, *30*, 3210−3216. (d) Su, X.; Baker, J. J.; Martin, C. D. Dimeric boroles: effective sources of monomeric boroles for heterocycle synthesis. *Chem. Sci.* **2020**, *11*, 126−131.

(3) (a) Köster, R.; Benedikt, G. 9-Borafluorenes. *Angew. Chem., Int. Ed.* **1963**, *2*, 323−324. (b) Eisch, J. J.; Hota, N. K.; Kozima, S. Synthesis of pentaphenylborole, a potentially antiaromatic system. *J. Am. Chem. Soc.* **1969**, *91*, 4575−4577. (c) Eisch, J. J.; Galle, J. E.; Kozima, S. Bora-aromatic systems. Part 8. The physical and chemical consequences of cyclic conjugation in boracyclopolyenes. The antiaromatic character of pentaarylboroles. *J. Am. Chem. Soc.* **1986**, *108*, 379−385. (d) Grigsby, W. J.; Power, P. P. Isolation and Reduction of Sterically Encumbered Arylboron Dihalides: Novel Boranediyl Insertion into C−C σ-Bonds. *J. Am. Chem. Soc.* **1996**, *118*, 7981−7988. (e) Wehmschulte, R. J.; Khan, M. A.; Twamley, B.; Schiemenz, B. Synthesis and Characterization of a Sterically Encumbered Unsymmetrical 9-Borafluorene, Its Pyridine Adduct, and Its Dilithium Salt. *Organometallics* **2001**, *20*, 844−849. (f) Yamaguchi, S.; Shirasaka, T.; Akiyama, S.; Tamao, K. Dibenzoborole-Containing π-Electron Systems: Remarkable Fluorescence Change Based on the "On/Off" Control of the pπ−π* Conjugation. *J. Am. Chem. Soc.* **2002**, *124*, 8816−8817. (g) Wehmschulte, R. J.; Diaz, A. A.; Khan, M. A. Unsymmetrical 9-Borafluorenes via Low-Temperature C−H Activation of *m*-Terphenylboranes. *Organometallics* **2003**, *22*, 83−92. (h) Braunschweig, H.; Fernández, I.; Frenking, G.; Kupfer, T. Structural Evidence for Antiaromaticity in Free Boroles. *Angew. Chem., Int. Ed.* **2008**, *47*, 1951−1954. (i) Adams, I. A.; Rupar, P. A. A Poly(9-Borafluorene) Homopolymer: An Electron-Deficient Polyfluorene with "Turn-On" Fluorescence Sensing of NH_3 Vapor. *Macromol. Rapid Commun.* **2015**, *36*, 1336−1340. (j) Smith, M. F.; Cassidy, S. J.; Adams, I. A.; Vasiliu, M.; Gerlach, D. L.; Dixon, D. A.; Rupar, P. A. Substituent Effects on the Properties of Borafluorenes. *Organometallics* **2016**, *35*, 3182−3191. (k) Ando, N.; Yamada, T.; Narita, H.; Oehlmann, N. N.; Wagner, M.; Yamaguchi, S. Boron-Doped Polycyclic π-Electron Systems with an Antiaromatic Borole Substructure That Forms Photoresponsive B−P Lewis Adducts. *J. Am. Chem. Soc.* **2021**, *143*, 9944−9951.

(4) (a) Entwistle, C. D.; Marder, T. B. Applications of Three-Coordinate Organoboron Compounds and Polymers in Optoelectronics. *Chem. Mater.* **2004**, *16*, 4574−4585. (b) Yamaguchi, S.; Wakamiya, A. Boron as a key component for new π-electron materials. *Pure Appl. Chem.* **2006**, *78*, 1413−1424. (c) Jäkle, F. Advances in the Synthesis of Organoborane Polymers for Optical, Electronic, and Sensory Applications. *Chem. Rev.* **2010**, *110*, 3985−4022. (d) Berger, C. J.; He, G.; Merten, C.; McDonald, R.; Ferguson, M. J.; Rivard, E. Synthesis and Luminescent Properties of Lewis Base-Appended Borafluorenes. *Inorg. Chem.* **2014**, *53*, 1475−1486. (e) Escande, A.; Ingleson, M. J. Fused polycyclic aromatics incorporating boron in the core: fundamentals and applications. *Chem. Commun.* **2015**, *51*, 6257−6274. (f) Ji, L.; Griesbeck, S.; Marder, T. B. Recent developments in and perspectives on three-coordinate boron materials: a bright future. *Chem. Sci.* **2017**, *8*, 846−863. (g) Su, X.; Bartholome, T. A.; Tidwell, J. R.; Pujol, A.; Yruegas, S.; Martinez, J. J.; Martin, C. D. 9-Borafluorenes: Synthesis, Properties, and Reactivity. *Chem. Rev.* **2021**, *121*, 4147−4192.

(5) Barnard, J. H.; Yruegas, S.; Huang, K.; Martin, C. D. Ring expansion reactions of anti-aromatic boroles: a promising synthetic avenue to unsaturated boracycles. *Chem. Commun.* **2016**, *52*, 9985−9991.

(6) (a) Biswas, S.; Maichle-Mössmer, C.; Bettinger, H. F. Rearrangement from the heteroantiaromatic borole to the heteroaromatic azaborine motif. *Chem. Commun.* **2012**, *48*, 4564−4566. (b) Barnard, J. H.; Brown, P. A.; Shuford, K. L.; Martin, C. D. 1,2-Phosphaborines: Hybrid Inorganic/Organic P−B Analogues of Benzene. *Angew. Chem., Int. Ed.* **2015**, *54*, 12083−12086. (c) Braunschweig, H.; Krummenacher, I.; Mailänder, L.; Rauch, F. O,N,B-Containing eight-membered heterocycles by ring expansion of boroles with nitrones. *Chem. Commun.* **2015**, *51*, 14513−14515. (d) Huang, K.; Couchman, S. A.; Wilson, D. J. D.; Dutton, J. L.; Martin, C. D. Reactions of Imines, Nitriles, and Isocyanides with Pentaphenylborole: Coordination, Ring Expansion, C−H Bond Activation, and Hydrogen Migration Reactions. *Inorg. Chem.* **2015**, *54*, 8957−8968. (e) Huang, K.; Martin, C. D. Ring Expansion Reactions of Pentaphenylborole with Dipolar Molecules as a Route to Seven-Membered Boron Heterocycles. *Inorg. Chem.* **2015**, *54*, 1869−1875. (f) Barnard, J. H.; Yruegas, S.; Couchman, S. A.; Wilson, D. J. D.; Dutton, J. L.; Martin, C. D. Reactivity of a Phosphaalkyne with Pentaarylboroles. *Organometallics* **2016**, *35*, 929−931. (g) Huang, K.; Martin, C. D. Peculiar Reactivity of Isothiocyanates with Pentaphenylborole. *Inorg. Chem.* **2016**, *55*, 330−337. (h) Shoji, Y.; Tanaka, N.; Muranaka, S.; Shigeno, N.; Sugiyama, H.; Takenouchi, K.; Hajjaj, F.; Fukushima, T. Boron-mediated sequential alkyne insertion and C−C coupling reactions affording extended π-conjugated molecules. *Nat. Commun.* **2016**, *7*, No. 12704. (i) Yruegas, S.; Martin, C. D. Expedient Synthesis of 1,2-Thiaborines by Means of Sulfur Insertion into Boroles. *Chem. - Eur. J.* **2016**, *22*, 18358−18361. (j) Adiraju, V. A. K.; Martin, C. D. Isomer Dependence on the Reactivity of Diazenes with Pentaphenylborole. *Chem. - Eur. J.* **2017**, *23*, 11437−11444. (k) Yruegas, S.; Wilson, C.; Dutton, J. L.; Martin, C. D. Ring Opening of Epoxides Induced by Pentaphenylborole. *Organometallics* **2017**, *36*, 2581−2587. (l) Bluer, K. R.; Laperriere, L. E.; Pujol, A.; Yruegas, S.; Adiraju, V. A. K.; Martin, C. D. Coordination and Ring Expansion of 1,2-Dipolar Molecules with 9-Phenyl-9-borafluorene. *Organometallics* **2018**, *37*, 2917−2927. (m) Shoji, Y.; Shigeno, N.; Takenouchi, K.; Sugimoto, M.; Fukushima, T. Mechanistic Study of Highly Efficient Direct 1,2-Carboboration of Alkynes with 9-Borafluorenes. *Chem. - Eur. J.* **2018**, *24*, 13223−13230. (n) Yruegas, S.; Barnard, J. H.; Al-Furaiji, K.; Dutton, J. L.; Wilson, D. J. D.; Martin, C. D. Boraphosphaalkene Synthesis via Phosphaalkyne Insertion into 9-Borafluorene. *Organometallics* **2018**, *37*, 1515−1518. (o) Bartholome, T. A.; Bluer, K. R.; Martin, C. D. Successive carbene insertion into 9-phenyl-9-borafluorene. *Dalton Trans.* **2019**, *48*, 6319−6322. (p) Kashida, J.; Shoji, Y.; Fukushima, T. Synthesis and Reactivity of Cyclic Borane-Amidine Conjugated Molecules Formed by Direct 1,2-Carboboration of Carbodiimides with 9-Borafluorenes. *Chem. - Asian J.* **2019**, *14*, 1879−1885. (q) Yang, W.; Krantz, K. E.; Dickie, D. A.; Molino, A.; Wilson, D. J. D.; Gilliard, R. J., Jr. Crystalline BP-Doped Phenanthryne via Photolysis of The Elusive Boraphosphaketene. *Angew. Chem., Int. Ed.* **2020**, *59*, 3971−3975. (r) Hagspiel, S.; Fantuzzi, F.; Dewhurst, R. D.; Gärtner, A.; Lindl, F.; Lamprecht, A.; Braunschweig, H. Adducts of the Parent Boraphosphaketene H_2BPCO and their Decarbonylative Insertion Chemistry. *Angew. Chem., Int. Ed.* **2021**, *60*, 13666−13670. (s) Lindl, F.; Guo, X.; Krummenacher, I.; Rauch, F.; Rempel, A.; Paprocki, V.; Dellermann, T.; Stennett, T. E.; Lamprecht, A.; Brückner, T.; et al. Rethinking Borole Cycloaddition Reactivity. *Chem. - Eur. J.* **2021**, *27*, 11226−11233.

(7) (a) Liu, L.; Marwitz, A. J. V.; Matthews, B. W.; Liu, S.-Y. Boron Mimetics: 1,2-Dihydro-1,2-azaborines Bind inside a Nonpolar Cavity of T4 Lysozyme. *Angew. Chem., Int. Ed.* **2009**, *48*, 6817−6819. (b) Knack, D. H.; Marshall, J. L.; Harlow, G. P.; Dudzik, A.; Szaleniec, M.; Liu, S.-Y.; Heider, J. BN/CC Isosteric Compounds as Enzyme Inhibitors: N- and B-Ethyl-1,2-azaborine Inhibit Ethylbenzene Hydroxylation as Nonconvertible Substrate Analogues. *Angew. Chem., Int. Ed.* **2013**, *52*, 2599−2601. (c) Wang, X.-Y.; Lin, H.-R.; Lei, T.; Yang, D.-C.; Zhuang, F.-D.; Wang, J.-Y.; Yuan, S.-C.; Pei, J. Azaborine Compounds for Organic Field-Effect Transistors: Efficient Synthesis, Remarkable Stability, and BN Dipole Interactions. *Angew. Chem., Int. Ed.* **2013**, *52*, 3117−3120. (d) Rombouts, F. J. R.; Tovar, F.; Austin, N.; Tresadern, G.; Trabanco, A. A. Benzazaborinines as Novel Bioisosteric Replacements of Naphthalene: Propranolol as an Example. *J. Med. Chem.* **2015**, *58*, 9287−9295. (e) Vlasceanu, A.; Jessing, M.; Kilburn, J. P. BN/CC isosterism in borazaronaphthalenes towards phosphodiesterase 10A (PDE10A) inhibitors. *Bioorg. Med. Chem.* **2015**, *23*, 4453−4461. (f) Wang, X.-Y.; Wang, J.-Y.; Pei, J. BN Heterosuperbenzenes: Synthesis and Properties. *Chem. - Eur. J.* **2015**, *21*, 3528−3539. (g) Morgan, M. M.; Piers, W. E. Efficient synthetic

https://doi.org/10.1021/acs.inorgchem.2c00930
Inorg. Chem. 2022, 61, 9595−9604

methods for the installation of boron−nitrogen bonds in conjugated organic molecules. *Dalton Trans.* **2016**, *45*, 5920−5924. (h) Wang, J.-Y.; Pei, J. BN-embedded aromatics for optoelectronic applications. *Chin. Chem. Lett.* **2016**, *27*, 1139−1146. (i) Giustra, Z. X.; Liu, S.-Y. The State of the Art in Azaborine Chemistry: New Synthetic Methods and Applications. *J. Am. Chem. Soc.* **2018**, *140*, 1184−1194. (j) von Grotthuss, E.; John, A.; Kaese, T.; Wagner, M. Doping Polycyclic Aromatics with Boron for Superior Performance in Materials Science and Catalysis. *Asian J. Org. Chem.* **2018**, *7*, 37−53. (k) Zhang, W.; Li, G.; Xu, L.; Zhuo, Y.; Wan, W.; Yan, N.; He, G. 9,10-Azaboraphenanthrene-containing small molecules and conjugated polymers: synthesis and their application in chemodosimeters for the ratiometric detection of fluoride ions. *Chem. Sci.* **2018**, *9*, 4444−4450. (l) Liu, Y.; Liu, S.-Y. Exploring the strength of a hydrogen bond as a function of steric environment using 1,2-azaborine ligands and engineered T4 lysozyme receptors. *Org. Biomol. Chem.* **2019**, *17*, 7002−7006. (m) Yan, N.; Zhang, W.; Li, G.; Zhang, S.; Yang, X.; Zhou, K.; Pei, D.; Zhao, Z.; He, G. AIE-active 9,10-azaboraphenanthrene-containing viologens for reversible electrochromic and electrofluorochromic applications. *Mater. Chem. Front.* **2021**, *5*, 4128−4137. (n) Gu, Y.; Muñoz-Mármol, R.; Fan, W.; Han, Y.; Wu, S.; Li, Z.; Bonal, V.; Villalvilla, J. M.; Quintana, J. A.; Boj, P. G.; et al. Peri-Acenoacene for Solution Processed Distributed Feedback Laser: The Effect of 1,2-Oxaborine Doping. *Adv. Opt. Mater.* **2022**, *10*, No. 2102782.

(8) (a) Braunschweig, H.; Hörl, C.; Mailänder, L.; Radacki, K.; Wahler, J. Antiaromaticity to Aromaticity: From Boroles to 1,2-Azaborinines by Ring Expansion with Azides. *Chem. - Eur. J.* **2014**, *20*, 9858−9861. (b) Couchman, S. A.; Thompson, T. K.; Wilson, D. J. D.; Dutton, J. L.; Martin, C. D. Investigating the ring expansion reaction of pentaphenylborole and an azide. *Chem. Commun.* **2014**, *50*, 11724−11726. (c) Müller, M.; Maichle-Mössmer, C.; Bettinger, H. F. BN-Phenanthryne: Cyclotetramerization of an 1,2-Azaborine Derivative. *Angew. Chem., Int. Ed.* **2014**, *53*, 9380−9383. (d) Braunschweig, H.; Celik, M. A.; Hupp, F.; Krummenacher, I.; Mailänder, L. Formation of BN Isosteres of Azo Dyes by Ring Expansion of Boroles with Azides. *Angew. Chem., Int. Ed.* **2015**, *54*, 6347−6351. (e) Braunschweig, H.; Hupp, F.; Krummenacher, I.; Mailänder, L.; Rauch, F. Ring Expansions of Boroles with Diazo Compounds: Steric Control of C or N Insertion and Aromatic/Nonaromatic Products. *Chem. - Eur. J.* **2015**, *21*, 17844−17849. (f) Braunschweig, H.; Celik, M. A.; Dellermann, T.; Frenking, G.; Hammond, K.; Hupp, F.; Kelch, H.; Krummenacher, I.; Lindl, F.; Mailänder, L.; et al. Scope of the Thermal Ring-Expansion Reaction of Boroles with Organoazides. *Chem. - Eur. J.* **2017**, *23*, 8006−8013. (g) Yruegas, S.; Martinez, J. J.; Martin, C. D. Intermolecular insertion reactions of azides into 9-borafluorenes to generate 9,10-B,N-phenanthrenes. *Chem. Commun.* **2018**, *54*, 6808−6811. (h) Lindl, F.; Lin, S.; Krummenacher, I.; Lenczyk, C.; Stoy, A.; Müller, M.; Lin, Z.; Braunschweig, H. 1,2,3-Diazaborinine: A BN Analogue of Pyridine Obtained by Ring Expansion of a Borole with an Organic Azide. *Angew. Chem., Int. Ed.* **2019**, *58*, 338−342.

(9) Yruegas, S.; Patterson, D. C.; Martin, C. D. Oxygen insertion into boroles as a route to 1,2-oxaborines. *Chem. Commun.* **2016**, *52*, 6658−6661.

(10) Kirschner, S.; Bao, S.-S.; Fengel, M. K.; Bolte, M.; Lerner, H.-W.; Wagner, M. Aryl−aryl coupling in a polycyclic aromatic hydrocarbon with embedded tetracoordinate boron centre. *Org. Biomol. Chem.* **2019**, *17*, 5060−5065.

(11) Romero, P. E.; Piers, W. E.; Decker, S. A.; Chau, D.; Woo, T. K.; Parvez, M. η^1 versus η^5 Bonding Modes in Cp*Al(I) Adducts of 9-Borafluorenes. *Organometallics* **2003**, *22*, 1266−1274.

(12) Motomura, T.; Hideko, N.; Michinori, S.; Masahiro, M.; Yoshihiko, I. Synthesis and Structural Analysis of Oligo(naphthalene-2,3-diyl)s. *Bull. Chem. Soc. Jpn.* **2005**, *78*, 142−146.

(13) Yruegas, S.; Axtell, J. C.; Kirlikovali, K. O.; Spokoyny, A. M.; Martin, C. D. Synthesis of 9-borafluorene analogues featuring a three-dimensional 1,1′-bis(*o*-carborane) backbone. *Chem. Commun.* **2019**, *55*, 2892−2895.

(14) The acceptor number (AN) is calculated by the equation, AN = 2.21 × (δ_{sample} − 41.0).

(15) When we conducted the reaction with 1 equivalent or 1.5 equivalents of PhN_3, the isolated yields of **4** were 21 and 26%, respectively.

(16) Ochiai, M.; Nakanishi, A.; Suefuji, T. Unprecedented Direct Oxygen Atom Transfer from Hypervalent Oxido-λ^3-iodanes to α,β-Unsaturated Carbonyl Compounds: Synthesis of α,β-Epoxy Carbonyl Compounds. *Org. Lett.* **2000**, *2*, 2923−2926.

(17) Epstein, W. W.; Sweat, F. W. Dimethyl Sulfoxide Oxidations. *Chem. Rev.* **1967**, *67*, 247−260.

(18) Rajkiewicz, A. A.; Wojciechowska, N.; Kalek, M. N-Heterocyclic Carbene-Catalyzed Synthesis of Ynones via C−H Alkynylation of Aldehydes with Alkynyliodonium Salts—Evidence for Alkynyl Transfer via Direct Substitution at Acetylenic Carbon. *ACS Catal.* **2020**, *10*, 831−841.

(19) Menzel, R.; Rapp, W. Excited singlet- and triplet-absorptions of pentaphene. *Chem. Phys.* **1984**, *89*, 445−455.

(20) Brouwer, A. M. Standards for photoluminescence quantum yield measurements in solution (IUPAC Technical Report). *Pure Appl. Chem.* **2011**, *83*, 2213−2228.

(21) (a) Sheldrick, G. M. A short history of SHELX. *Acta Crystallogr., Sect. A: Found. Crystallogr.* **2008**, *64*, 112−122. (b) Dolomanov, O. V.; Bourhis, L. J.; Gildea, R. J.; Howard, J. A. K.; Puschmann, H. OLEX2: a complete structure solution, refinement and analysis program. *J. Appl. Crystallogr.* **2009**, *42*, 339−341.

(22) (a) Becke, A. D. Density-functional thermochemistry. III. The role of exact exchange. *J. Chem. Phys.* **1993**, *98*, 5648−5652. (b) Weigend, F.; Ahlrichs, R. Balanced basis sets of split valence, triple zeta valence and quadruple zeta valence quality for H to Rn: Design and assessment of accuracy. *Phys. Chem. Chem. Phys.* **2005**, *7*, 3297−3305. (c) Weigend, F. Accurate Coulomb-fitting basis sets for H to Rn. *Phys. Chem. Chem. Phys.* **2006**, *8*, 1057−1065. (d) Grimme, S.; Antony, J.; Ehrlich, S.; Krieg, H. A consistent and accurate ab initio parametrization of density functional dispersion correction (DFT-D) for the 94 elements H-Pu. *J. Chem. Phys.* **2010**, *132*, No. 154104. (e) Neese, F. Software update: The ORCA program system—Version 5.0. *Wiley Interdiscip. Rev.: Nanomed. Nanobiotechnol.* **2022**, No. e1606.

(23) (a) Barone, V.; Cossi, M. Quantum Calculation of Molecular Energies and Energy Gradients in Solution by a Conductor Solvent Model. *J. Phys. Chem. A* **1998**, *102*, 1995−2001. (b) Cossi, M.; Rega, N.; Scalmani, G.; Barone, V. Energies, structures, and electronic properties of molecules in solution with the C-PCM solvation model. *J. Comput. Chem.* **2003**, *24*, 669−681.

(24) (a) Stanger, A. Nucleus-Independent Chemical Shifts (NICS): Distance Dependence and Revised Criteria for Aromaticity and Antiaromaticity. *J. Org. Chem.* **2006**, *71*, 883−893. (b) Frisch, M. J.; et al. *Gaussian 16*, revision C.01; Gaussian Inc.: Wallingford, CT, 2016.

(25) (a) Keith, T. A.; Bader, R. F. W. Calculation of magnetic response properties using atoms in molecules. *Chem. Phys. Lett.* **1992**, *194*, 1−8. (b) Geuenich, D.; Hess, K.; Köhler, F.; Herges, R. Anisotropy of the Induced Current Density (ACID), a General Method To Quantify and Visualize Electronic Delocalization. *Chem. Rev.* **2005**, *105*, 3758−3772.

(26) Yanai, T.; Tew, D. P.; Handy, N. C. A new hybrid exchange−correlation functional using the Coulomb-attenuating method (CAM-B3LYP). *Chem. Phys. Lett.* **2004**, *393*, 51−57.

(27) Berraud-Pache, R.; Neese, F.; Bistoni, G.; Izsák, R. Unveiling the Photophysical Properties of Boron-dipyrromethene Dyes Using a New Accurate Excited State Coupled Cluster Method. *J. Chem. Theory Comput.* **2020**, *16*, 564−575.

https://doi.org/10.1021/acs.inorgchem.2c00930
Inorg. Chem. 2022, 61, 9595−9604